$G_{s\alpha}$ meets its target – shedding light on a key signal transduction event

John J Dumas and David G Lambright*

The recently determined crystal structure of $G_{s\alpha}$ bound to a catalytically active form of adenylyl cyclase reveals the location of the enzyme's active site and provides the first view of heterotrimeric G protein α subunit activating a downstream effector. Comparison with the structure of a catalytically inactive form of adenylyl cyclase suggests a plausible allosteric mechanism whereby the synergistic activators $G_{s\alpha}$ and forskolin stimulate the activity of adenylyl cyclase.

Address: Program in Molecular Medicine, University of Massachusetts Medical Center, 373 Plantation Street, Worcester, MA 01605, USA.

*Corresponding author.
E-mail: David.Lambright@ummed.edu

Structure 15 April 1998, **6**:407–411
http://biomednet.com/elecref/0969212600600407

The mechanisms by which extracellular signals modulate levels of intracellular second messengers have been the subject of intense biochemical investigation since the discovery of the first known second messenger, cyclic AMP, in the 1950s [1]. Over the last five years, crystallographic studies have begun to unravel the structural basis of G-protein-coupled signaling. The latest crystallographic milestone represents the culmination of years of detailed biochemical analyses combined with a clever strategy to convert the membrane-bound form of adenylyl cyclase (AC), the enzyme responsible for synthesis of cAMP, into a soluble enzyme that retained both catalytic activity and the ability to be modulated by forskolin — a plant terpenoid known to directly activate AC — and G proteins. In the December 12th issue of *Science*, Tesmer *et al.* report the crystal structure of a complex consisting of the soluble catalytic domains of AC, activated by forskolin and the GTP-bound α subunit of G_s, the heterotrimeric G protein ($G_{\alpha\beta\gamma}$) that activates AC [2].

Heptahelical receptors, which are activated by ligand binding, catalyze the exchange of GTP for GDP on the α subunits of heterotrimeric G proteins. The conformational switch induced by GTP binding activates G_α subunits and promotes the release of $G_{\beta\gamma}$. The activity of a variety of downstream effectors, typically ion channels or enzymes that generate second messengers, has been shown to be modulated by G_α·GTP or the released $G_{\beta\gamma}$. Perhaps the most intensively studied G-protein target is AC, the membrane-bound enzyme that converts ATP into the intracellular second messenger cAMP. To date, ten different isoforms of AC have been identified [3,4]. Although differences exist with respect to regulation by $G_{\beta\gamma}$ subunits and the inhibitory G protein, $G_{i\alpha}$, all ten isoforms are activated by $G_{s\alpha}$ and forskolin, and are inhibited by analogues of adenosine (P-site inhibitors) in the presence of pyrophosphate and Mg^{2+}. ACs have two homologous cytoplasmic domains, designated C1 and C2, which resemble domains found in guanylyl cyclases. Each of these cytoplasmic domains can be independently expressed as a soluble homodimer, capable of binding two molecules of forskolin but lacking catalytic activity. A key biochemical breakthrough was the expression of soluble, catalytically active, C1–C2 fusion proteins [5]. Gilman and colleagues later showed that the inactive C1 and C2 homodimers, when mixed together, spontaneously form C1–C2 heterodimers, possessing both catalytic activity and the ability to be stimulated by forskolin and GTP-bound $G_{s\alpha}$ [6,7]. Moreover, functional heterodimers could also be obtained by mixing the C1 and C2 domains from different isoforms. Indeed, it was just one such heterodimer (VC1–IIC2; the Roman numerals designate the isoform) that was used in the crystallographic studies of Tesmer *et al.* [2].

Orientation with respect to the membrane

Figure 1 shows the structure of $G_{s\alpha}$ bound to the C1–C2 heterodimer of AC. The location of the N terminus of $G_{s\alpha}$ (reversibly palmitoylated *in vivo*), as well as the N and C termini of the C1 and C2 domains, orients the 'dorsal' face of the C1–C2 heterodimer toward the membrane surface and the membrane spanning segments of adenylyl cyclase. In this proposed orientation, the cleft between the two domains on the 'ventral' surface of the heterodimer is roughly parallel to the plane of the membrane, so that the forskolin-binding site and the active site face the cytoplasm. The various membrane-associated modulators of AC, including $G_{s\alpha}$, $G_{i\alpha}$ and $G_{\beta\gamma}$, would then be constrained to interact with peripheral regions of the C1–C2 heterodimer remote from the enzyme active site. On the basis of studies which indicate that $G_{i\alpha}$ and $G_{s\alpha}$ do not compete for binding to AC [8], Tesmer *et al.* propose that the binding site for $G_{i\alpha}$ might be located opposite that for $G_{s\alpha}$, between the α3 helix and the α1–α2 loop of the C1 domain. The binding of $G_{s\alpha}$ and $G_{i\alpha}$ to pseudosymmetric sites may help to explain how $G_{i\alpha}$ selectively inhibits a subset of AC isoforms, whereas $G_{s\alpha}$ activates all isoforms

Locating the active site

The overall structure of the C1–C2 heterodimer is similar to that of the C2 homodimer. The C2 homodimer binds two molecules of forskolin in a dyad symmetric arrangement,

Figure 1

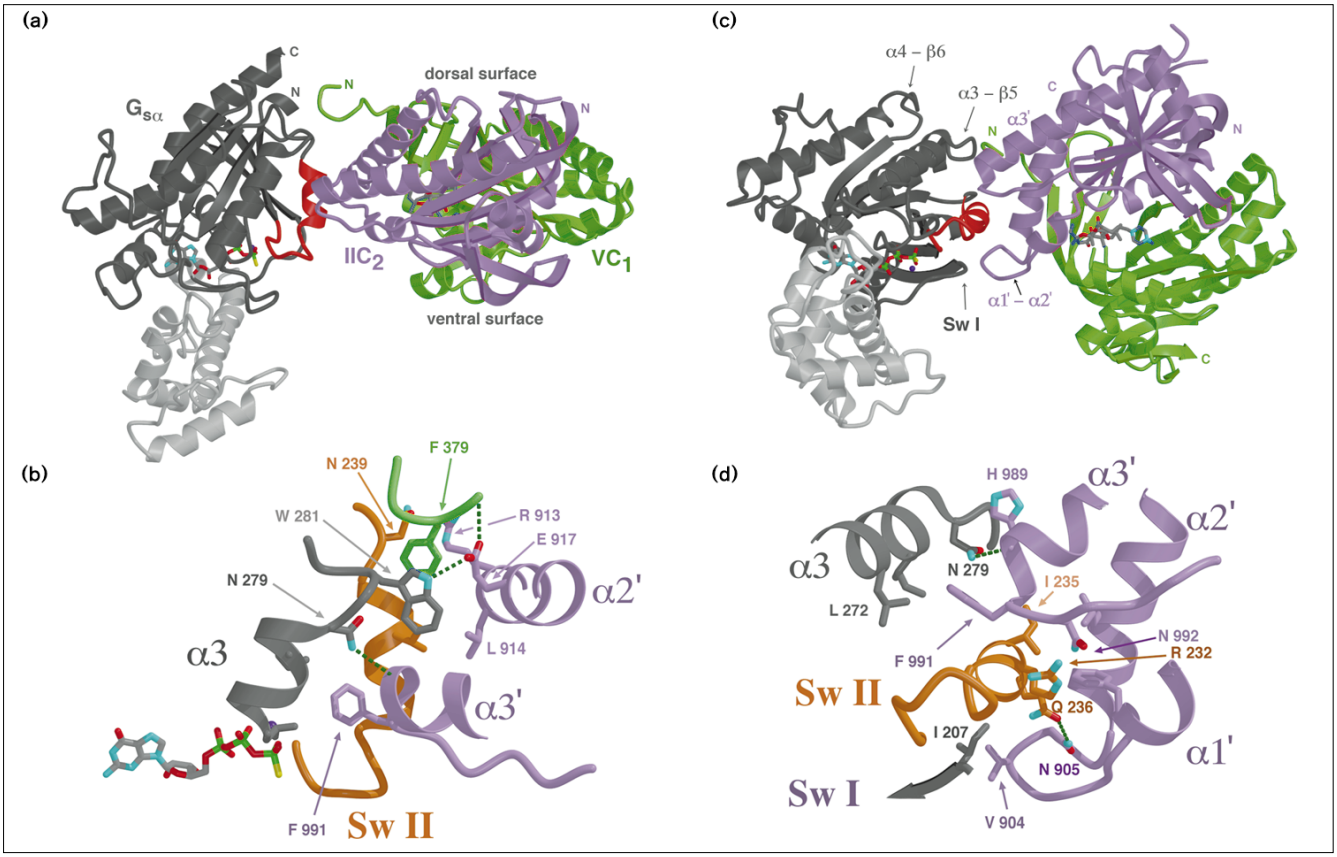

The complex of $G_{s\alpha}$·GTPγS and the C1–C2 heterodimer of adenylyl cyclase. The ras-like domain of $G_{s\alpha}$ is shown in dark grey; the helical domain in light grey; and the switch II domain (Sw II) in red. Adenylyl cyclase (AC) fragment VC1 is shown in green and IIC2 in purple. **(a)** N termini are presumed to be oriented toward the lipid bilayer, thus the 'dorsal surface' of AC faces the membrane, whereas the ventral surface faces the cytoplasm. **(b)** Detailed view showing Sw II of $G_{s\alpha}$ (same orientation as above) and the regions of C1–C2 with which it interacts. **(c)** The complex of $G_{s\alpha}$·GTPγS and C1–C2 rotated about the horizontal axis by 70° relative to (a). **(d)** Detailed view showing the interface between $G_{s\alpha}$ and C1–C2, in the same orientation as (c). (Figure reproduced from [2] with permission.)

with the binding sites situated at opposite ends of the shallow ventral cleft formed at the interface between the two domains [9]. In contrast, only a single molecule of forskolin is bound to the pseudosymmetric C1–C2 heterodimer (Figure 2) [2]. Comparison of the forskolin-binding site with the pseudosymmetric site reveals two key amino acid differences that explain how a second molecule of forskolin is excluded from binding to the C1–C2 heterodimer. Asn1025 and Asp440 in the pseudosymmetric site replace Thr512 and Ser942, respectively, in the forskolin-binding site. The sidechains of both asparagine and aspartate would sterically prohibit binding of a second molecule of forskolin to this site. Although the potential steric clash with Asn1025 could be alleviated by rotation of the C1 domain to coincide with the corresponding domain in the C2 homodimer, the predicted steric clash with Asp440 would remain.

To locate the binding site for P-site inhibitors, Tesmer *et al.* soaked native crystals with a P-site inhibitor consisting of 2′,d3′-AMP, pyrophosphate and Mg^{2+}. Interestingly, the P-site inhibitor binds to a site that is pseudosymmetric with the forskolin-binding site and at the opposite end of the ventral cleft from the $G_{s\alpha}$-binding site. Like the forskolin-binding site, the P-site is formed by structural elements from both the C1 and C2 domains. The pyrophosphate moiety is situated near a strand–loop–helix element structurally reminiscent of the P-loop common to nucleotide-binding proteins and interacts with the Mg^{2+} ion and three basic residues. Mg^{2+} binds with apparent octahedral geometry and four of six expected ligands are visible in the structure, including two aspartic acid residues (Asp396 and Asp440), a mainchain carbonyl oxygen (Ile397) and a β-phosphate oxygen of the pyrophosphate group. The remaining sites are presumably occupied by water molecules.

Binding studies [10], as well as the structure of the complex [2], suggest that P-site inhibitors bind to the same site as the substrate, exerting their inhibitory effect by mimicking

Figure 2

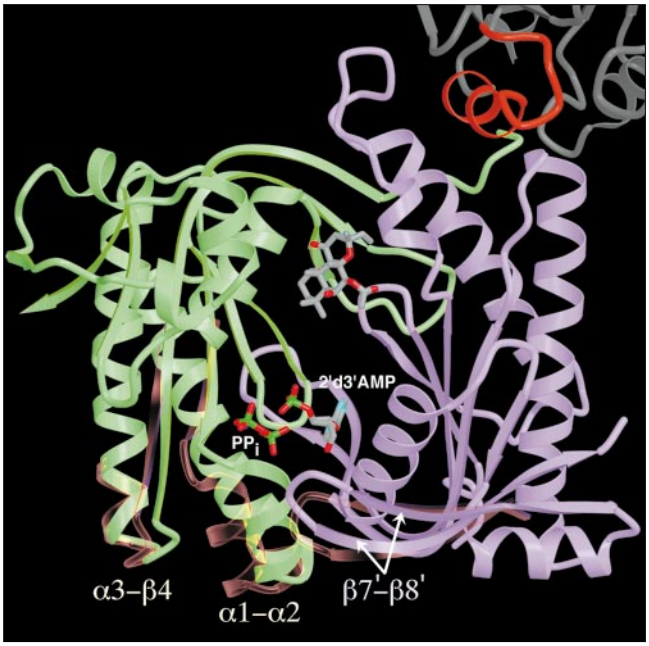

The binding sites of the P-site inhibitors, forskolin and ATP on the ventral surface of the C1–C2 heterodimer. 2′,d3′-AMP and pyrophosphate of the P-site inhibitor are bound in the ventral cleft of C1–C2 at the end furthest from the site of interaction with $G_{s\alpha}$. Forskolin binds to a site that is pseudosymmetric to the P-site. Regions of the C1–C2 heterodimer which have a different conformation in the absence of the P-site inhibitor are shown in transparent pink. (Figure reproduced from [2] with permission.)

the products of the reaction, cAMP and pyrophosphate. Because it was not possible to locate the substrate-binding site by soaking native crystals with the non-hydrolyzable ATP analogue $Ap(CH_2)pp$, Tesmer *et al.* constructed a model for ATP bound in the active site using the location of the 2′,d3′-AMP, pyrophosphate and Mg^{2+} of the P-site inhibitor complex to position the corresponding elements of ATP. The resulting conformation of ATP places the 3′ OH group of the ribose moiety in a favorable orientation for in-line attack of the α-phosphate group (Figures 3a and b). This model also explains why mutation of Arg1029 reduces

Figure 3

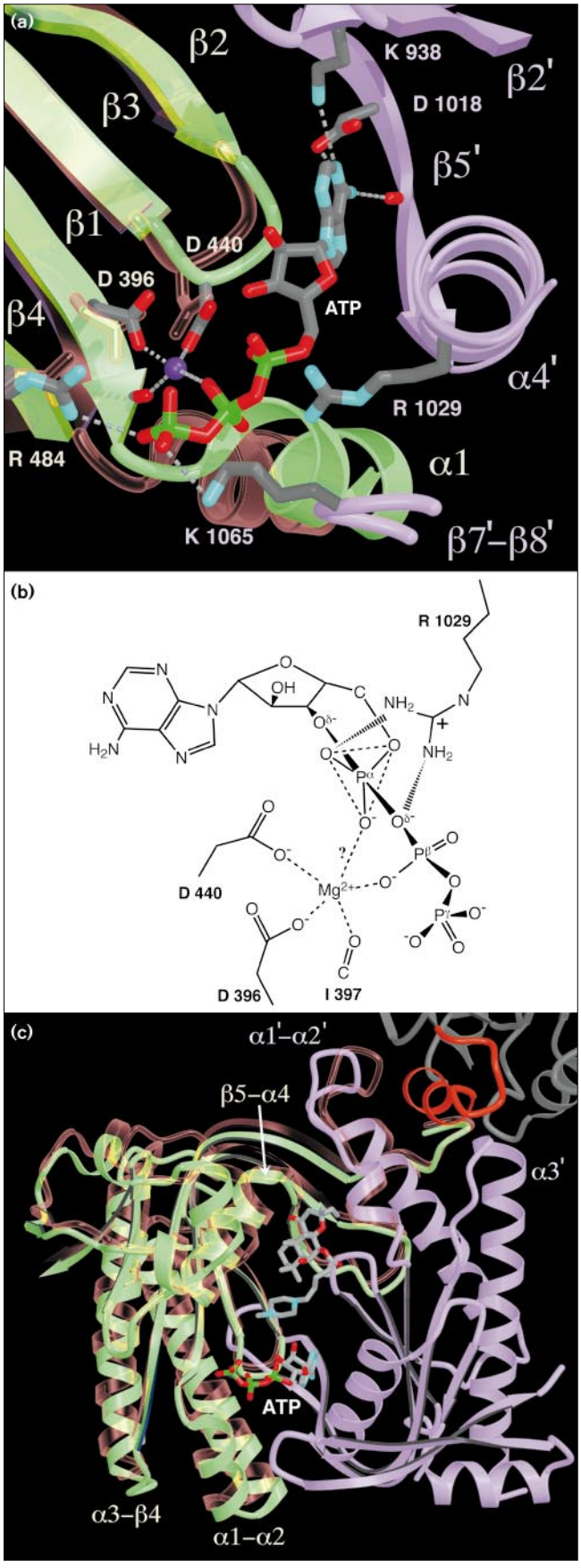

The mechanism of $G_{s\alpha}$ activation of the C1–C2 heterodimer. **(a)** Model of ATP·Mg^{2+} bound to the catalytic site of VC1–IIC2. The unactivated heterodimer (based upon structure of the IIC2 homodimer) is shown in transparent pink and the activated C1–C2 is solid green. The position of ATP is modeled on the basis of the position of 2′,d3′-AMP and pyrophosphate in the active site. **(b)** Schematic diagram of the putative transition state for GTP hydrolysis in which Arg1029 stabilizes the pentavalent phosphate intermediate. **(c)** Model of the conformational changes accompanying AC activation by $G_{s\alpha}$. Binding of $G_{s\alpha}$ results in a 7° rotation of the C1 domain with respect to C2; color coding as for (a). (Figure reproduced from [2] with permission.)

Figure 4

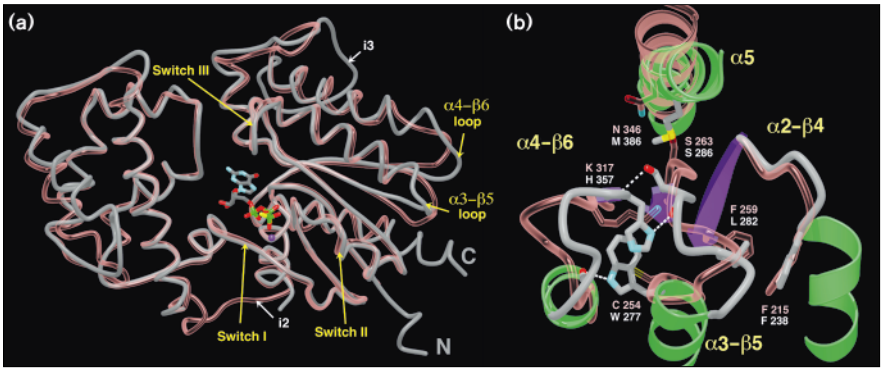

Comparison of the structures of the $G_{s\alpha}$ (grey) and $G_{i\alpha}$ (pink). **(a)** The structure of $G_{s\alpha}$·GTPγS is superimposed on that of $G_{i\alpha}$. The most notable divergence is seen in the α3–β5 and α4–β6 loops. **(b)** The putative effector-binding loops (α2–β4, α3–β5 and α4–β6) and the α5 helix of $G_{s\alpha}$ superimposed on the corresponding elements of $G_{i\alpha}$. (Figure reproduced from [16] with permission.)

k_{cat} but has no effect on K_m: the guanidylyl group of Arg1029 is located near the α-phosphate group of ATP and is predicted to stabilize the transition state in a manner reminiscent of the conserved catalytic arginine in heterotrimeric G protein α subunits and the 'arginine finger' of GTPase-activating proteins that stabilize the transition state for GTP hydrolysis [11–14].

The interface between $G_{s\alpha}$ and adenylyl cyclase

The interaction between $G_{s\alpha}$ and the C1–C2 domains of AC buries 1800 Å^2 of solvent accessible surface area in a single contiguous interface. All but a handful of $G_{s\alpha}$ residues that contribute to this interaction are located in either the switch II region (specifically the α2 helix and α2–β4 turn) or in the adjacent α3–β5 loop. Interestingly, contacts between C1–C2 and residues within the α4–β6 loop of $G_{s\alpha}$ are not observed. Scanning-mutagenesis experiments, in which residues of $G_{s\alpha}$ were replaced with corresponding residues from $G_{i\alpha}$, indicated that the α4–β6 loop of $G_{s\alpha}$ is important for interaction with AC [15]. One explanation for this apparent conundrum is that the α4–β6 loop interacts with a region of the cytoplasmic face of AC, which lies outside the C1 and C2 domains. An alternative and perhaps simpler explanation is that the conformations of the α3–β5 and α4–β6 loops are mutually dependent. Substitutions within the α4–β6 loop might therefore alter the conformation of key residues in the α3–β5 loop, which in turn interact directly with AC. Indeed, as Sunahara *et al.* observe, the primary and tertiary structures of these loops differ substantially between $G_{i\alpha}$ and $G_{s\alpha}$ [16]. Moreover, the conformations of these loops in $G_{s\alpha}$ are stabilized by hydrogen-bonding and stacking interactions involving Trp277 and His357 (Figure 4).

Mechanism of adenylyl cyclase activation

How is the binding of $G_{s\alpha}$ at a relatively small interface at one end of the C1–C2 dimer communicated to the active site some 30 Å away? Evidently, a global conformational change is required. The conformational change induced by $G_{s\alpha}$ and/or forskolin binding, however, does not alter significantly the K_m of ATP or the K_i for $Ap(CH_2)pp$, but rather reorients catalytic residues to accelerate the rate of cAMP formation. To deduce a plausible model for the nature of the conformational change leading to cyclase activation, Tesmer *et al.* compare the structure of forskolin- and $G_{s\alpha}$-activated C1–C2 heterodimer with that of the inactive C2 homodimer (Figure 3c). $G_{s\alpha}$ appears to activate AC by inserting its α2 (switch II) helix into a shallow cleft formed by the α3′ helix and α1′–α2′ loop of the C2 domain. The α1′–α2′ loop is displaced by 3 Å relative to the α3′ helix. These changes are transduced to the C1 domain through an extensive interface centered on the β5–α4 region, leading to a small but significant global rotation of the C1 domain that repositions key active-site residues.

The road ahead

The most important unresolved question about this signaling pathway — how an activated receptor activates a heterotrimeric G protein — also poses some of the greatest biochemical hurdles: expression, purification, solubilization and crystallization of an integral membrane receptor. However, with recent success on two crucial fronts — the high level expression of the α-factor receptor in yeast [17] and the atomic resolution structure of bacteriorhodopsin crystallized from lipidic cubic phases [18] — an atomic level description of heterotrimeric G protein signaling, from receptor to effector, seems almost within reach.

Acknowledgements

We thank Stephen Sprang for kindly providing original images for the figures.

References

1. Sutherland, E.W. (1972). Studies on the mechanism of hormone action. *Science* **177**, 401-408.
2. Tesmer, J.J., Sunahara, R.K., Gilman, A.G. & Sprang, S.R. (1997). Crystal structure of the catalytic domains of adenylyl cyclase in a complex with $G_{s\alpha}$·GTPγS. *Science* **278**, 1907-1916.
3. Iyengar, R. (1993). Molecular and functional diversity of mammalian G_s-stimulated adenylyl cyclases. *FASEB J.* **7**, 768-775.
4. Sunahara, R.K., Dessauer, C.W. & Gilman, A.G. (1996). Complexity and diversity of mammalian adenylyl cyclases. *Annu. Rev. Pharmacol. Toxicol.* **36**, 461-480.

5. Tang, W.J. & Gilman, A.G. (1995). Construction of a soluble adenylyl cyclase activated by $G_{s\alpha}$ and forskolin. *Science* **268**, 1769-1772.
6. Dessauer, C.W. & Gilman, A.G. (1996). Purification and characterization of a soluble form of mammalian adenylyl cyclase. *J. Biol. Chem.* **271**, 16967-16974.
7. Whisnant, R.E., Gilman, A.G. & Dessauer, C.W. (1996). Interaction of the two cytosolic domains of mammalian adenylyl cyclase. *Proc. Natl. Acad. Sci. USA* **93**, 6621-6625.
8. Taussig, R., Tang, W.J., Hepler, J.R. & Gilman, A.G. (1994). Distinct patterns of bidirectional regulation of mammalian adenylyl cyclases. *J. Biol. Chem.* **269**, 6093-6100.
9. Zhang, G., Liu, Y., Ruoho, A.E. & Hurley, J.H. (1997). Structure of the adenylyl cyclase catalytic core. *Nature* **386**, 247-253.
10. Dessauer, C.W., Scully, T.T. & Gilman, A.G. (1997). Interactions of forskolin and ATP with the cytosolic domains of mammalian adenylyl cyclase. *J. Biol. Chem.* **272**, 22272-22277.
11. Sondek, J., Lambright, D.G., Noel, J.P., Hamm, H.E. & Sigler, P.B. (1994). GTPase mechanism of G proteins from the 1.7 Å crystal structure of transducin α-GDP–AlF_4^-. *Nature* **372**, 276-279.
12. Tesmer, J.J., Berman, D.M., Gilman, A.G. & Sprang, S.R. (1997). Structure of RGS4 bound to AlF4-activated $G_{i\alpha1}$: stabilization of the transition state for GTP hydrolysis. *Cell* **89**, 251-261.
13. Scheffzek, K., *et al*., Wittinghofer, A. (1997). The ras–rasGAP complex: structural basis for GTPase activation and its loss in oncogenic ras mutants. *Science* **277**, 333-338.
14. Rittinger, K., Walker, P.A., Eccleston, J.F., Smerdon, S.J. & Gamblin S.J. (1997). Structure at 1.65 Å of RhoA and its GTPase-activating protein in complex with a transition-state analogue. *Nature* **389**, 758-762.
15. Berlot, C.H. & Bourne, H.R. (1992). Identification of effector-activating residues of $G_{s\alpha}$. *Cell* **68**, 911-922.
16. Sunahara, R.K., Tesmer, J.J., Gilman A.G. & Sprang S.R. (1997). Crystal structure of the adenylyl cyclase activator $G_{s\alpha}$. *Science* **278**, 1943-1947.
17. David, N.E., Gee, M., Andersen, B., Naider, F., Thorner, J. & Stevens, R.C. (1997). Expression and purification of the *Saccharomyces cerevisiae* α-factor receptor (Ste2p), a 7-transmembrane-segment G protein-coupled receptor. *J. Biol. Chem.* **272**, 15553-15561.
18. Pebay-Peyroula, E., Rummel, G., Rosenbusch, J.P. & Landau, E.M. (1997). X-ray structure of bacteriorhodopsin at 2.5 Å from microcrystals grown in lipidic cubic phases. *Science* **277**, 1676-1681.